Interaction network of SARS-CoV-2 with host receptome through spike protein

Yunqing Gu [1, 8], Jun Cao [1, 2, 8], Xinyu Zhang [1, 8], Hai Gao [1, 3, 8], Yuyan Wang [4, 8], Jia Wang [5, 8], Jinlan Zhang [1], Guanghui Shen [2], Xiaoyi Jiang [1], Jie Yang [1], Xichen Zheng [1, 2], Jianqing Xu [1, 6], Cheng Cheng Zhang [7], Fei Lan [1], Di Qu [4], Yun Zhao [5], Guoliang Xu [1, 5], Youhua Xie [1, 4, *], Min Luo [1,2, *], Zhigang Lu [1, *]

[1] The Fifth People's Hospital of Shanghai, the Shanghai Key Laboratory of Medical Epigenetics, the International Co-laboratory of Medical Epigenetics and Metabolism, Ministry of Science and Technology, Institutes of Biomedical Sciences, Fudan University, Shanghai 200032, China

[2] Institute of Pediatrics of Children's Hospital of Fudan University, Shanghai 201102, China

[3] Zhongshan-Xuhui Hospital, Fudan Univeristy, Shanghai 200020, China

[4] Key Laboratory of Medical Molecular Virology (MOE/MOH), School of Basic Medical Sciences, Shanghai Medical College, Fudan University, Shanghai 200032, China

[5] State Key Laboratory of Molecular Biology, CAS Center for Excellence in Molecular Cell Science, Institute of Biochemistry and Cell Biology, Shanghai Institutes for Biological Sciences, Chinese Academy of Sciences, Shanghai 200031, China

[6] Shanghai Public Health Clinical Center, Fudan University, Shanghai 200433, China

[7] Department of Physiology, University of Texas Southwestern Medical Center, Dallas, TX 75390, USA

[8] These authors contributed equally to this work.

* Corresponding author. Email: zhiganglu@fudan.edu.cn (Z.L.); luo_min@fudan.edu.cn (M.L.); yhxie@fudan.edu.cn (Y.X.).

SUMMARY

Host cellular receptors are key determinants of virus tropism and pathogenesis. Virus utilizes multiple receptors for attachment, entry, or specific host responses. However, other than ACE2, little is known about SARS-CoV-2 receptors. Furthermore, ACE2 cannot easily interpret the multi-organ tropisms of SARS-CoV-2 nor the clinical differences between SARS-CoV-2 and SARS-CoV. To identify host cell receptors involved in SARS-CoV-2 interactions, we performed genomic receptor profiling to screen almost all human membrane proteins, with SARS-CoV-2 capsid spike (S) protein as the target. Twelve receptors were identified, including ACE2. Most receptors bind at least two domains on S protein, the receptor-binding-domain (RBD) and the N-terminal-domain (NTD), suggesting both are critical for virus-host interaction. Ectopic expression of ASGR1 or KREMEN1 is sufficient to enable entry of SARS-CoV-2, but not SARS-CoV and MERS-CoV. Analyzing single-cell transcriptome profiles from COVID-19 patients revealed that virus susceptibility in airway epithelial ciliated and secretory cells and immune macrophages highly correlates with expression of ACE2, KREMEN1 and ASGR1 respectively, and ACE2/ASGR1/KREMEN1 (ASK) together displayed a much better correlation than any individual receptor. Based on modeling of systemic SARS-CoV-2 host interactions through S receptors, we revealed ASK correlation with SARS-CoV-2 multi-organ tropism and provided potential explanations for various COVID-19 symptoms. Our study identified a panel of SARS-CoV-2 receptors with diverse binding properties, biological functions, and clinical correlations or implications, including ASGR1 and KREMEN1 as the alternative entry receptors, providing insights into critical interactions of SARS-CoV-2 with host, as well as a useful resource and potential drug targets for COVID-19 investigation.

MAIN TEXT

The global outbreak of COVID-19 caused by SARS-CoV-2 severely threatens human health [1,2]. SARS-CoV-2 is a member of the beta-coronavirus genus, closely related to severe acute respiratory syndrome coronavirus (SARS-CoV), and both viruses use ACE2 as an entry receptor [3-5]. SARS-CoV-2 is more than a respiratory virus, with multi-organ tropisms and causing complicated symptoms [2,6-8]. Host cellular receptors play key roles in determining virus tropism and pathogenesis. Viruses bind to multiple host receptors for viral attachment, cell entry, and diverse specific host responses, including inducing cytokine secretion, stimulation of the immune response, or alteration of virus budding and release [9-12]. However, apart from ACE2, little is known about SARS-CoV-2 receptors. Additionally, ACE2 cannot fully interpret SARS-CoV-2 tropism. The virus was detected in tissues with few ACE2 expression, such as liver, brain and blood, and even in lung, only a small subset of cells express ACE2 [13,14]. The primary infection sites and clinical manifestations of SARS-CoV-2 and SARS-CoV also differ much, suggesting the involvement of other receptor(s) in SARS-CoV-2 host interaction [1,2,15-18]. Therefore, a comprehensive understanding of SARS-CoV-2 cellular receptors is required.

Identification of receptors from virus-susceptible cells is limited to membrane proteins on specific cell types. We previously investigated ligand-receptor interactions using a cell based method, in which receptor-expressing cells were incubated with a tagged ligand and then an anti-tag for labelling and detection [19,20]. It closely reassembles ligand-receptor interaction that occurring under physiological condition, and is usually used to confirm specific interactions. Based on this method, we developed a high-throughput receptor profiling system covering nearly all human membrane proteins, and used it to identify SARS-CoV-2 cellular receptors. Given SARS-CoV-2 S protein is the major receptor binding protein on the virus capsid, we performed profilling using S protein as the target. 5054 human membrane protein-encoding genes (91.6% of predicted

human membrane proteins) were expressed individually on human 293e cells, and their binding with the extracellular domain of S protein (S-ECD) was measured (Fig. 1a). Twelve membrane proteins were identified that specifically interact with the S-ECD (Fig. 1b, c and Extended Data Fig.1), including the previously reported ACE2 [4,5] and SARS-CoV-specific CLEC4M (L-SIGN) [21].

The dissociation constants (Kd) of these interactions ranged from 12.4 - 525.4 nM (Table.1 and Extended Data Fig.2). ACE2 binds to S-ECD with a Kd of 12.4 nM, comparable to the previously reported Kd [22], and ACE2, CD207, CLEC4M, and KREMEN1 are all high-affinity receptors of the S protein, with comparable Kds. Binding domains on S protein were also examined, including the receptor binding domain (RBD), N-terminal domain (NTD) and S2 domain. The RBD and NTD are the major binding sites of S receptors. ACE2 only binds to the RBD, while CD207 and ERGIC3 bind exclusively with the NTD. The other receptors can bind to at least two domains, with CLEC4M, KREMEN1, and LILRB2 binding to all three domains, showing highest binding with NTD, RBD, and RBD, respectively (Table.1 and Extended Data Fig.3). Overall, these receptors showed diverse binding patterns, and they have a diverse range of biological functions and signaling properties (Extended Data Fig.4).

To determine whether these receptors can mediate virus entry independent of ACE-2, ACE2 was further knocked out in the HEK293T cell line (Extended Data Fig.5), which is low-sensitive to SARS-CoV-2 and SARS-CoV [3,4,16]. We ectopically expressed the receptors in ACE2-KO 293T cells individually, and infected cells separately with pseudotyped SARS-CoV-2, SARS-CoV or MERS-CoV. KREMEN1-expressing cells showed clear evidence of SARS-CoV-2 infection, as did ASGR1, although to a lesser extent (Fig. 2a). Both receptors are specific to SARS-CoV-2, whereas ACE2 mediates the entry of both SARS-CoV-2 and SARS-CoV (Fig. 2a). ASGR1- and KREMEN1-dependent virus entry was confirmed with patient-derived SARS-CoV-2, with ASGR1

102 promoting higher levels of infection (Fig. 2b, c).

103 Direct interaction of SARS-CoV-2 S protein with KREMEN1 and ASGR1 was
104 confirmed by co-immuno-precipitation (Co-IP) (Fig. 2d). KREMEN1 and ASGR1 bind to
105 S-ECD with Kds of 19.3 nM and 94.8 nM, respectively, the former Kd being comparable
106 to that of ACE2 (12.4 nM). ACE2 has the highest maximum binding capacity for S-ECD,
107 being ~3- and ~10-fold that of ASGR1 and KREMEN1, respectively (Fig. 2e), consistent
108 with the SARS-CoV-2 sensitivities of cells expressing these receptors (Fig. 2a-c). Few
109 binding of SARS-CoV S protein was observed with ASGR1 and KREMEN1 (Fig. 2e and
110 Extended Data Fig.6), consistent with KREMEN1 and ASGR1 not mediating SARS-CoV
111 infections (Fig. 2a). ACE2 binds exclusively to the RBD, KREMEN1 binds to all three
112 domains of S-ECD, and with highest binding to the RBD, and ASGR1 binds to both the
113 NTD and the RBD, the latter also with higher binding (Table. 1 and Extended Data Fig.3).
114 Evidence indicates that the NTD is involved in entry coronavirus including SARS-CoV-2
115 [23-26], suggesting the potential importance of ASGR1 and KREMEN1 in SARS-CoV-2
116 infection. KREMEN1 is a high-affinity DKK1 receptor that antagonizes canonical WNT
117 signaling [27], and is also the entry receptor for a major group of Enteroviruses [28]. ASGR1
118 is an endocytic recycling receptor that plays a critical role in serum glycoprotein
119 homeostasis [29] and has been reported to facilitate entry of Hepatitis C virus [30]. Thus,
120 ASGR1 and KREMEN1 directly mediate SARS-CoV-2 entry, together with ACE2, we
121 refer to them as the ASK (ACE2/ASGR1/KREMEN1) entry receptors.

122 To investigate the clinical relevance of these entry receptors for SARS-CoV-2
123 susceptibility, we analyzed a recently published single cell sequencing (scRNA-seq)
124 profile of the upper respiratory tract of 19 patients with COVID-19 [31]. The dataset was
125 derived from nasopharyngeal/pharyngeal swabs, and contains both the gene expression
126 and virus infection status for individual cells, which are composed mainly of epithelial
127 and immune populations. ACE2 is principally expressed in epithelial populations, as

128 previously reported [31], whereas ASGR1 and KREMEN1 are enriched in both epithelial
129 and immune populations (Fig. 3a). The majority of ASK^+ cells express only one entry
130 receptor (88.5%), and KREMEN1-expressing cells are the most abundant, being ~5-fold
131 more numerous than either ACE2- or ASGR1-expressing cells (Fig. 3b and Extended
132 Data Fig.7a). SARS-CoV-2 is mainly observed in epithelial ciliated and secretory cells
133 and immune non-resident macrophages (nrMa), which are also the major populations that
134 express ASK receptors (Fig. 3b, c). Within SARS-CoV-2 positive cells (V^+ cells), only
135 10.3% expressed ACE-2, suggesting other receptors will facilitate entry (Fig. 3c and
136 Extended Data Fig.8).

137 We determined the correlation of the KREMEN1, ASGR1, and ACE2 entry receptors
138 with SARS-CoV-2 susceptibility. In total cells, the receptor-positive cell percentage was
139 significantly higher in V^+ cells than in V^- cells for all three receptors (Fig. 3d). In
140 epithelial populations, both ACE2 and KREMEN1 were substantially enriched in V^+ cells,
141 while in immune populations, only ASGR1 correlated with virus susceptibility, especially
142 in macrophages (Fig. 3d and Extended Data Fig.7b). The epithelial ciliated and secretory
143 cells are known target cells of SARS-CoV-2 [14,31]. ACE2 displayed a more significant
144 correlation with the virus susceptibility of ciliated cells when compared with KREMEN1,
145 which was the only entry receptor that highly correlates virus susceptibility in secretory
146 cells. Either in all cells or cell subpopulations, the ASK combination was usually more
147 highly correlated with virus infection than individual receptors (Fig. 3d and Extended
148 Data Fig.7b).

149 SARS-CoV-2 displays multi-organ tropism in COVID-19 patients [6,12,13,17,32]. However,
150 in virus-positive tissues, such as brain, liver, peripheral blood (PB) and even lung, ACE2
151 expression is few or only detected in a small subset of cells [13,14,18] (Extended Data Fig.9a,
152 b), suggesting that ACE2 alone is difficult to explain the multi-organ tropisms of
153 SARS-CoV-2. To determine whether ASK expression can predict tissue tropism better

154 than ACE2 expression, we modeled a systemic host-SARS-CoV-2 interaction based on
155 the expression of ASK entry receptors across human tissues (Fig. 4a). For a better
156 comparison of different receptors from aspect of viral binding, the mRNA level was
157 normalized with the S binding affinity of each receptor. ACE2 and ASGR1 are highly
158 expressed in the gastrointestine and liver, respectively, while KREMEN1 is broadly
159 expressed throughout the body. In virus-positive tissues, we found least one of the entry
160 receptors is expressed (Extended Data Fig.9b and Fig. 4a). When ASK receptor
161 expression levels were correlated with virus infection rates in different tissues reported in
162 a recent biopsy study [6], the three receptors together correlated much better with virus
163 susceptibility than any individual receptor (Fig. 4b). These results suggest that ASK
164 expression underlies the multi-organ tropism of SARS-CoV-2, and is therefore can
165 potentially predict viral tropism.

166 Despite functioning in viral entry, virus-host receptor interactions could also induce
167 cytokine secretion, apoptosis, and stimulation of the immune response, or alter virus
168 budding and release [9-12]. To gain insight into SARS-CoV-2 pathogenesis, we also
169 modeled the host–SARS-CoV-2 interaction based on the tissue distribution of all the
170 other receptors identified, which were classified according to their functions in immune
171 regulation, the Wnt pathway, and protein trafficking. The interaction map revealed that
172 expression of immune receptors is prominent in immune organs, as well as respiratory
173 organs, and the liver (Extended Data Fig.9 and Fig. 4a), consistent with the respiratory
174 manifestation and frequent liver injury in COVID-19 patients [1,2,32,33] . Given that CD207,
175 CLEC4M, LILRB2 and SIGLEC9 all are mainly expressed in myeloid cells (Extended
176 Data Fig.10) and that COVID-19 is associated with hyperactivation of myeloid
177 populations [12,34,35], it is possible that these receptors may drive monocyte and macrophage
178 activation in COVID-19 and contribute to disease pathophysiology.

179 ERGIC3, LMAN2, and MGAT2, which are involved in protein trafficking, display an

180 approximately similar expression levels across most human tissues (Extended Data Fig.9
181 and Fig. 4c). ERGIC3 and LMAN2 are the components of the endoplasmic
182 reticulum-Golgi intermediate compartment (ERGIC), which is essential for coronavirus
183 assembly and budding [36 37], while LMAN2 and ERGIC1 were recently found to interact
184 specifically with nonstructural protein Nsp7 and Nsp10 of SARS-CoV-2 respectively [38].
185 Whether and how they cooperate during virus life cycle are worth further investigation.
186 Expression of receptors of the Wnt pathway group is prominent in salivary gland, tongue,
187 esophagus, and brain (Extended Data Fig.9 and Fig. 4c). Wnt/β-catenin signaling is
188 critical in taste bud cell renewal and behavioral taste perception [39,40] and KREMEN1/2
189 plus FUT8 are all negative regulators of this pathway [27,41]. Loss of smell and taste has
190 frequently been observed in COVID-19 patients [42,43], suggesting SARS-CoV-2 may act
191 through these receptors to affect Wnt/β-catenin signaling and therefore taste loss.

192 The affinity-based interactions between SARS-CoV-2 and cellular receptors are key
193 determinants of virus tropism and pathogenesis. Determining cells or tissues that express
194 receptors should allow better characterization of the pathway for virus infection and help
195 understand COVID-19 disease progression. Our genomic receptor profiling of most
196 human membrane proteins has identified two additional virus entry receptors, ASGR1
197 and KREMEN1, independent of known ACE2. The combined ASK expression pattern
198 predicts viral tropism much more closely than any individual entry receptor from cell to
199 tissue levels. Our results also suggested that SARS-CoV-2 entry into different type of
200 cells rely on different receptors, and ASK receptors underlie the tropism of SARS-CoV-2.
201 Notably, ASGR1 and KREMEN1 do not mediate the entry of SARS-CoV, plausibly
202 explaining the difference of these two viruses in primary infection sites and clinical
203 manifestations. Unlike ACE2, which only binds to the RBD, ASGR1 and KREMEN1
204 bind to both the RBD and NTD. NTD is implicated in coronavirus entry [25,26], and several
205 neutralizing antibodies from convalescent COVID-19 patients recognizes NTD [23,24],
206 suggesting that the domain plays a role during SARS-CoV-2 infection, and that

207 antibodies against the NTD may act through ASGR1 or KREMEN1.

208 The twelve SARS-CoV-2 receptors that bind S protein have diverse binding properties,
209 functions, and tissue distributions. Integrating this panel of receptors with virological and
210 clinical data should lead to the identification of infection and pathological mechanisms
211 and targets. It is plausible that alternative binding receptors exert context-dependent
212 regulatory effects, leading to differential signaling outcomes, ultimately influencing
213 infection patterns, immune responses and clinical progression. Our study provides insight
214 into critical virus-host interactions, tropisms, and pathogenesis of SARS-CoV-2, as well
215 as potential targets for drug development against COVID-19.

REFERENCES

1 Zhu, N. *et al.* A Novel Coronavirus from Patients with Pneumonia in China, 2019. *New Engl J Med* **382**, 727-733, doi:10.1056/NEJMoa2001017 (2020).

2 Huang, C., Wang, Y. & Li, X. Clinical features of patients infected with 2019 novel coronavirus in Wuhan, China (vol 395, pg 497, 2020). *Lancet* **395**, 496-496, doi:10.1016/S0140-6736(20)30252-X (2020).

3 Hoffmann, M. *et al.* SARS-CoV-2 Cell Entry Depends on ACE2 and TMPRSS2 and Is Blocked by a Clinically Proven Protease Inhibitor. *Cell* **181**, 271-280 e278, doi:10.1016/j.cell.2020.02.052 (2020).

4 Li, W. H. *et al.* Angiotensin-converting enzyme 2 is a functional receptor for the SARS coronavirus. *Nature* **426**, 450-454, doi:10.1038/nature02145 (2003).

5 Zhou, P. *et al.* A pneumonia outbreak associated with a new coronavirus of probable bat origin. *Nature* **579**, 270-+, doi:10.1038/s41586-020-2012-7 (2020).

6 Puelles, V. G. *et al.* Multiorgan and Renal Tropism of SARS-CoV-2. *N Engl J Med*, doi:10.1056/NEJMc2011400 (2020).

7 Gupta, A. *et al.* Extrapulmonary manifestations of COVID-19. *Nat Med* **26**, 1017-1032, doi:10.1038/s41591-020-0968-3 (2020).

8 Progress report on the coronavirus pandemic. *Nature* **584**, 325, doi:10.1038/d41586-020-02414-1 (2020).

9 Schneider-Schaulies, J. Cellular receptors for viruses: links to tropism and pathogenesis. *J Gen Virol* **81**, 1413-1429, doi:10.1099/0022-1317-81-6-1413 (2000).

10 Milone, M. C. & Fitzgerald-Bocarsly, P. The mannose receptor mediates induction of IFN-alpha in peripheral blood dendritic cells by enveloped RNA and DNA viruses. *J Immunol* **161**, 2391-2399 (1998).

11 Tseng, C. T., Perrone, L. A., Zhu, H., Makino, S. & Peters, C. J. Severe acute respiratory syndrome and the innate immune responses: modulation of effector cell function without productive infection. *J Immunol* **174**, 7977-7985, doi:10.4049/jimmunol.174.12.7977 (2005).

12 Tay, M. Z., Poh, C. M., Renia, L., MacAry, P. A. & Ng, L. F. P. The trinity of COVID-19: immunity, inflammation and intervention. *Nat Rev Immunol* **20**, 363-374, doi:10.1038/s41577-020-0311-8 (2020).

13 Hikmet, F. *et al.* The protein expression profile of ACE2 in human tissues. *Mol Syst Biol* **16**, e9610, doi:10.15252/msb.20209610 (2020).

14 Sungnak, W. *et al.* SARS-CoV-2 entry factors are highly expressed in nasal epithelial cells together with innate immune genes. *Nat Med* **26**, 681-687, doi:10.1038/s41591-020-0868-6 (2020).

15 Lukassen, S. *et al.* SARS-CoV-2 receptor ACE2 and TMPRSS2 are primarily expressed in bronchial transient secretory cells. *EMBO J* **39**, e105114, doi:10.15252/embj.20105114 (2020).

16 HinChu. Comparative tropism, replication kinetics, and cell damage profiling of SARS-CoV-2 and SARS-CoV with implications for clinical manifestations, transmissibility, and laboratory studies of COVID-19: an observational study. *Lancet Microbe* **1**, e14-23,

256 doi:https://doi.org/10.1016/S2666-5247(20)30004-5 (2020).
257 17 Zou, L. *et al.* SARS-CoV-2 Viral Load in Upper Respiratory Specimens of Infected Patients. *N*
258 *Engl J Med* **382**, 1177-1179, doi:10.1056/NEJMc2001737 (2020).
259 18 Hou, Y. J. *et al.* SARS-CoV-2 Reverse Genetics Reveals a Variable Infection Gradient in the
260 Respiratory Tract. *Cell* **182**, 429-446 e414, doi:10.1016/j.cell.2020.05.042 (2020).
261 19 Deng, M. *et al.* A motif in LILRB2 critical for Angptl2 binding and activation. *Blood* **124**, 924-935,
262 doi:10.1182/blood-2014-01-549162 (2014).
263 20 Zheng, J. *et al.* Inhibitory receptors bind ANGPTLs and support blood stem cells and leukaemia
264 development. *Nature* **485**, 656-660, doi:10.1038/nature11095 (2012).
265 21 Jeffers, S. A. *et al.* CD209L (L-SIGN) is a receptor for severe acute respiratory syndrome
266 coronavirus. *P Natl Acad Sci USA* **101**, 15748-15753, doi:10.1073/pnas.0403812101 (2004).
267 22 Wrapp, D. *et al.* Cryo-EM structure of the 2019-nCoV spike in the prefusion conformation.
268 *Science* **367**, 1260-1263, doi:10.1126/science.abb2507 (2020).
269 23 Liu, L. *et al.* Potent neutralizing antibodies against multiple epitopes on SARS-CoV-2 spike.
270 *Nature* **584**, 450-456, doi:10.1038/s41586-020-2571-7 (2020).
271 24 Chi, X. *et al.* A neutralizing human antibody binds to the N-terminal domain of the Spike protein
272 of SARS-CoV-2. *Science*, doi:10.1126/science.abc6952 (2020).
273 25 Lu, G., Wang, Q. & Gao, G. F. Bat-to-human: spike features determining 'host jump' of
274 coronaviruses SARS-CoV, MERS-CoV, and beyond. *Trends Microbiol* **23**, 468-478,
275 doi:10.1016/j.tim.2015.06.003 (2015).
276 26 Wang, N. *et al.* Structural Definition of a Neutralization-Sensitive Epitope on the MERS-CoV
277 S1-NTD. *Cell Rep* **28**, 3395-3405 e3396, doi:10.1016/j.celrep.2019.08.052 (2019).
278 27 Mao, B. *et al.* Kremen proteins are Dickkopf receptors that regulate Wnt/beta-catenin signalling.
279 *Nature* **417**, 664-667, doi:10.1038/nature756 (2002).
280 28 Staring, J. *et al.* KREMEN1 Is a Host Entry Receptor for a Major Group of Enteroviruses. *Cell*
281 *Host Microbe* **23**, 636-643 e635, doi:10.1016/j.chom.2018.03.019 (2018).
282 29 Seidah, N. G., Chretien, M. & Mbikay, M. The ever-expanding saga of the proprotein convertases
283 and their roles in body homeostasis: emphasis on novel proprotein convertase subtilisin kexin
284 number 9 functions and regulation. *Curr Opin Lipidol* **29**, 144-150,
285 doi:10.1097/MOL.0000000000000484 (2018).
286 30 Saunier, B. *et al.* Role of the asialoglycoprotein receptor in binding and entry of hepatitis C virus
287 structural proteins in cultured human hepatocytes. *J Virol* **77**, 546-559,
288 doi:10.1128/jvi.77.1.546-559.2003 (2003).
289 31 Chua, R. L. *et al.* COVID-19 severity correlates with airway epithelium-immune cell interactions
290 identified by single-cell analysis. *Nat Biotechnol*, doi:10.1038/s41587-020-0602-4 (2020).
291 32 Xiao, F. *et al.* Evidence for Gastrointestinal Infection of SARS-CoV-2. *Gastroenterology* **158**,
292 1831-1833 e1833, doi:10.1053/j.gastro.2020.02.055 (2020).
293 33 Phipps, M. M. *et al.* Acute Liver Injury in COVID-19: Prevalence and Association with Clinical
294 Outcomes in a Large US Cohort. *Hepatology*, doi:10.1002/hep.31404 (2020).
295 34 Liao, M. *et al.* Single-cell landscape of bronchoalveolar immune cells in patients with COVID-19.
296 *Nat Med* **26**, 842-844, doi:10.1038/s41591-020-0901-9 (2020).

297 35 Zhou, Y. G. *et al.* Pathogenic T-cells and inflammatory monocytes incite inflammatory storms in
298 severe COVID-19 patients. *Natl Sci Rev* **7**, 998-1002, doi:10.1093/nsr/nwaa041 (2020).
299 36 Schoeman, D. & Fielding, B. C. Coronavirus envelope protein: current knowledge. *Virol J* **16**, 69,
300 doi:10.1186/s12985-019-1182-0 (2019).
301 37 Lontok, E., Corse, E. & Machamer, C. E. Intracellular targeting signals contribute to localization
302 of coronavirus spike proteins near the virus assembly site. *J Virol* **78**, 5913-5922,
303 doi:10.1128/JVI.78.11.5913-5922.2004 (2004).
304 38 Gordon, D. E. *et al.* A SARS-CoV-2 protein interaction map reveals targets for drug repurposing.
305 *Nature* **583**, 459-468, doi:10.1038/s41586-020-2286-9 (2020).
306 39 Gaillard, D. *et al.* beta-catenin is required for taste bud cell renewal and behavioral taste
307 perception in adult mice. *PLoS Genet* **13**, e1006990, doi:10.1371/journal.pgen.1006990 (2017).
308 40 Liu, F. *et al.* Wnt-beta-catenin signaling initiates taste papilla development. *Nat Genet* **39**, 106-112,
309 doi:10.1038/ng1932 (2007).
310 41 Kurimoto, A. *et al.* The absence of core fucose up-regulates GnT-III and Wnt target genes: a
311 possible mechanism for an adaptive response in terms of glycan function. *J Biol Chem* **289**,
312 11704-11714, doi:10.1074/jbc.M113.502542 (2014).
313 42 Menni, C. *et al.* Real-time tracking of self-reported symptoms to predict potential COVID-19. *Nat*
314 *Med* **26**, 1037-1040, doi:10.1038/s41591-020-0916-2 (2020).
315 43 Xydakis, M. S. *et al.* Smell and taste dysfunction in patients with COVID-19. *Lancet Infect Dis*,
316 doi:10.1016/S1473-3099(20)30293-0 (2020).

317

FIGURES

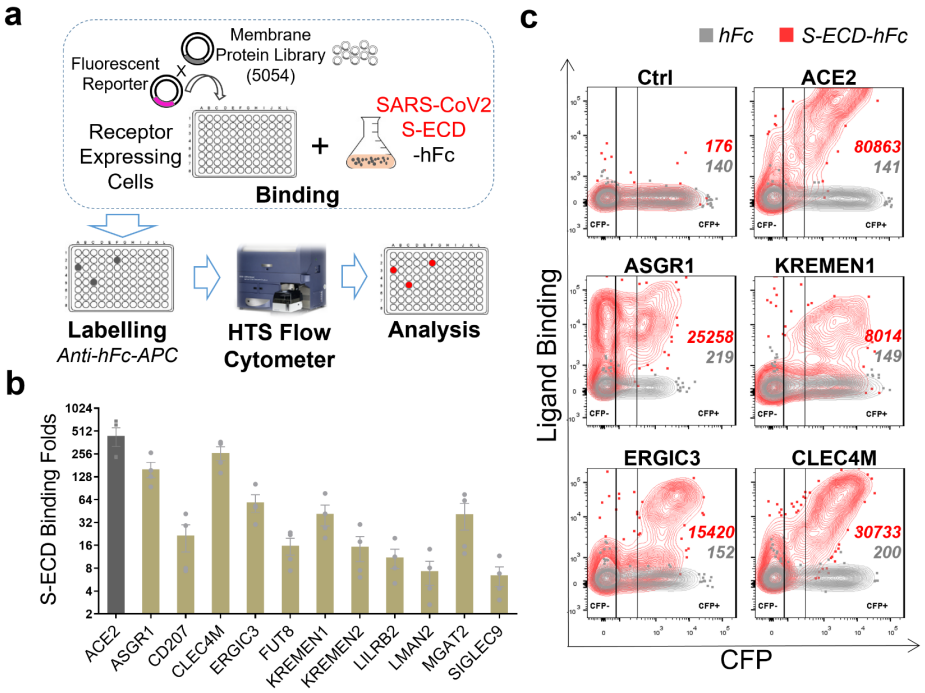

Figure 1: Genomic receptor profiling identifies twelve SARS-CoV-2 S binding receptors. a, Scheme of genomic receptor profiling. Plasmids encoding 5054 human membrane proteins were individually co-transfected with a CFP reporter into 293e cells. Cells were incubated with SARS-CoV-2 S-ECD-hFc protein, labelled using anti-hFc-APC antibody, binding was measured by flow cytometry. **b**, SIP identified S binding receptors. Relative binding of receptors with S-ECD-hFc compared to that with hFc control in CFP^{+} cells were shown. **c**, Representative flow dot plot showing the binding of S-ECD with top-ranking receptors.

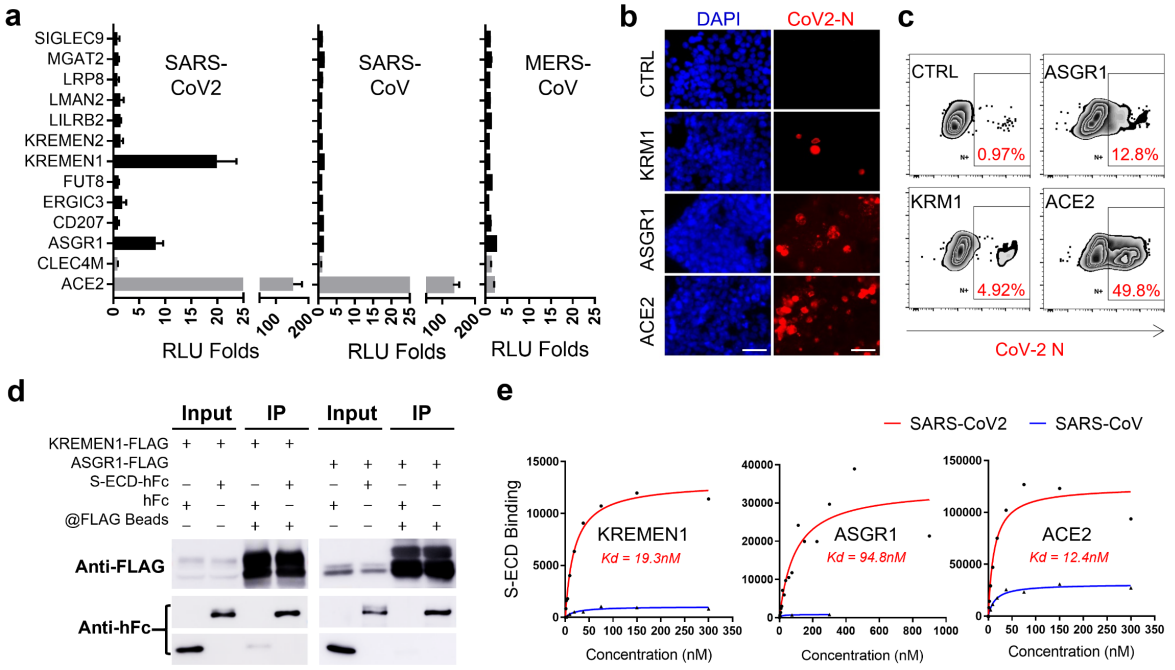

Figure 2. KREMEN1 and ASGR1 directly mediate SARS-CoV-2 entry. a, SIP-identified S-binding receptors were ectopically expressed in ACE2-KO 293T cells individually, followed by infection with pseudotyped SARS-CoV-2, SARS-CoV, and MERS-CoV separately. Luciferase activities relative to that of empty vector transfected cells were measured 60 hrs post infection. Data are presented as mean ± s.d (n=3). **b and c**, KREMEN1, ASGR1, or ACE2 transfected ACE2-KO 293T cells were infected with authentic SARS-CoV-2, and immune- fluorescence (B) or flow cytometry (C) were performed with antibody against the N protein of SARS-CoV-2 72hr post infection. Bar = 50μm. **d**, Co-immuno- precipitation was used to detect the interaction of S-ECD with full length KREMEN1 or ASGR1. **e**, KREMEN1, ASGR1 or ACE2 expressing 293e cells were incubated with different concentrations of S-ECD-hFc of SARS-CoV2 or SARS-CoV, separately, and S-ECD binding was monitored by flow cytometry to determine Kd.

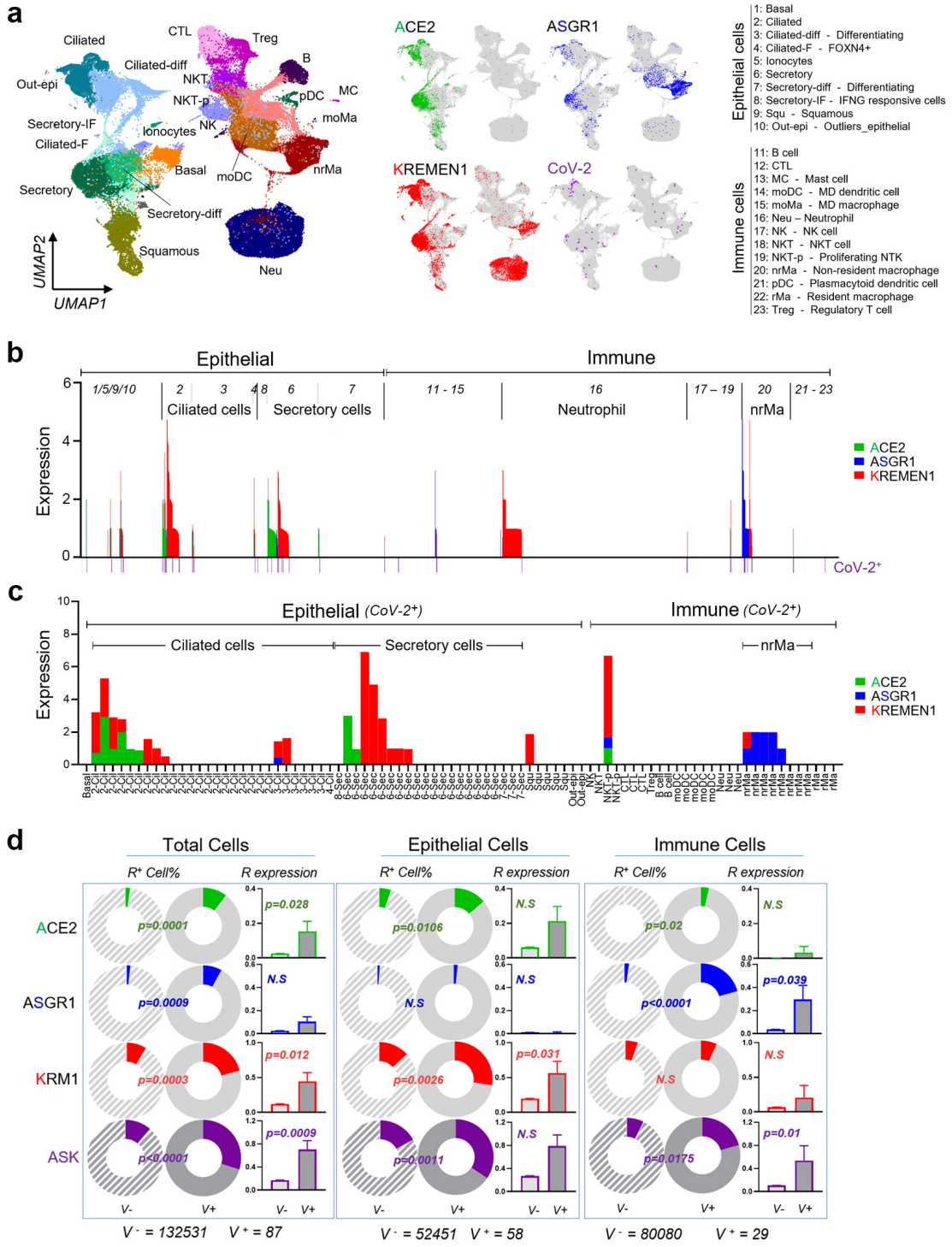

Figure 3. ASK entry receptors correlate significantly with SARS-CoV-2 susceptibility in the upper respiratory tract. a, Distribution of ACE2, ASGR1, KREMEN1 and SARS-CoV-2 in different cell populations of the upper airway. **b**,

349 Overlapping map of ASK expression levels and virus infection pattern in different cell
350 populations. **c**, ASK expression pattern in SARS-CoV-2 positive cells. **d**, Correlations of
351 virus susceptibility with ASK receptors individually or in combination based on receptor
352 positive cell percentage and receptor expression level.

353

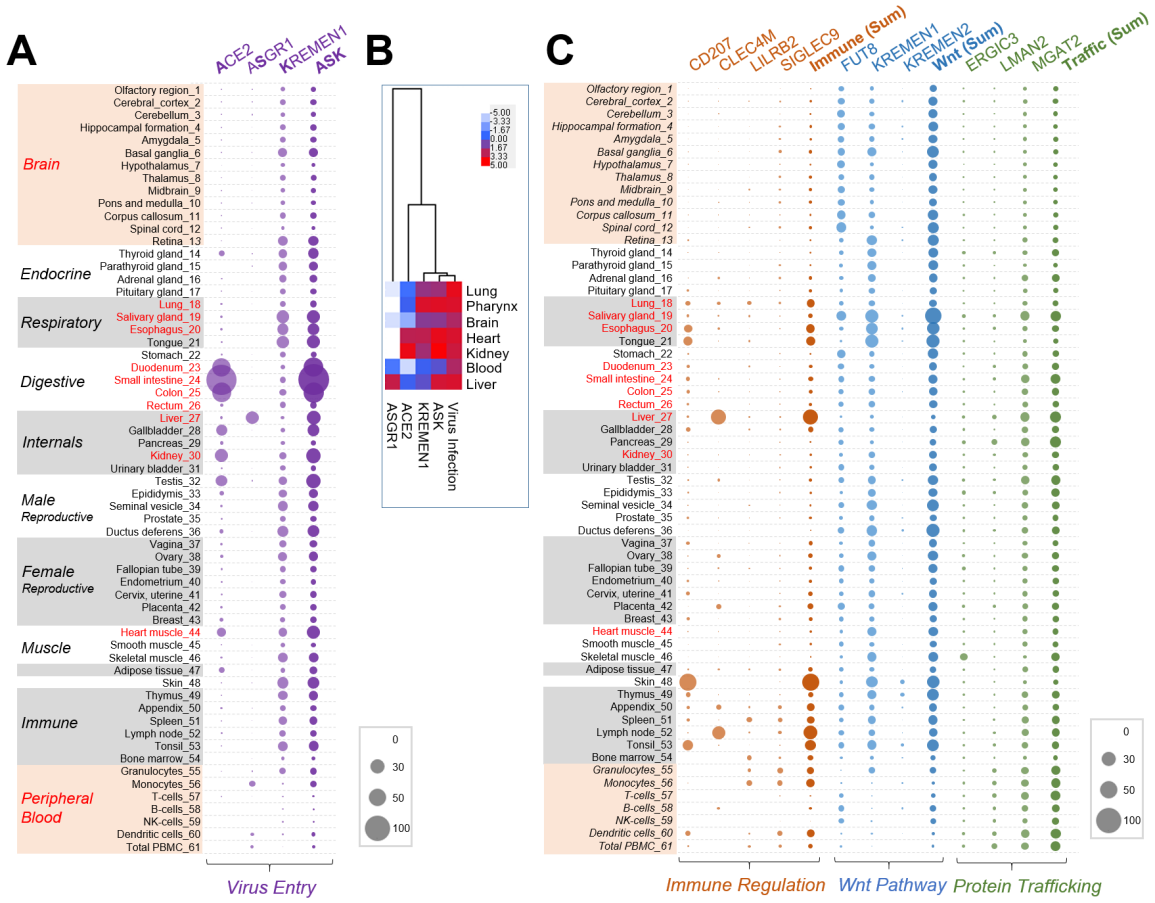

Figure 4. Systemic modeling of SARS-CoV-2 interactions within human tissues. The mRNA expression levels of each receptor in human tissues were derived from the human protein Atlas. Receptor-mediated SARS-CoV-2 binding potentials in each tissue were calculated by dividing receptor expression level with its affinity for S protein (Kd). **a**, Virus binding potentials of each tissue contributed by "entry group" ASK receptors. **b**, Virus infection rates (number of virus positive samples) in the indicated tissues were derived from a recent biopsy study [6], and these were clustered with ASK receptor-mediated virus binding potentials. **c**, Virus binding potentials of each tissue contributed by the S-binding receptors involved in immune regulation, the Wnt pathway and protein trafficking individually or in combination. In **a** and **c**, tissues or organs that were identified as positive to SARS-CoV-2 are labeled red.

367 **Table 1: Characteristics of the interaction between receptors and SARS-CoV-2 S**

368 **protein**

Gene Symbol	ACCN	MP Type	Kd Measurement		Relative Binding Folds		
			Kd (nM)	*Std.Error*	NTD	RBD	S2
ACE2	NM_021804	I	12.4	*3.8*		**493**	
ASGR1	NM_001671	II	94.8	*31.1*	38.9	**410**	
CD207	NM_015717	II	13.2	*2.8*	**8.9**		
CLEC4M	NM_014257	II	16.0	*3.3*	**63.6**	7.9	4.9
ERGIC3	NM_198398	Multi	525.4	*40.5*	**16.4**		
FUT8	NM_004480	II	34.9	*7.9*	**11.9**		2.7
KREMEN1	NM_001039571	I	19.3	*7.7*	4.2	**37.5**	5.5
KREMEN2	NM_172229	I	60.0	*14.2*		**14.0**	
LILRB2	NM_001080978	I	106.2	*28.1*	2.5	**24.3**	2.3
LMAN2	NM_006816	I	355.1	*46.8*			
MGAT2	NM_002408	II	36.3	*4.3*	**8.4**		4.1
SIGLEC9	NM_014441	I	116.5	*30.9*	3.0	**5.0**	

369 ACCN, Accession Number; MP Type, Membrane Protein Type.

370

371 **METHODS**

372 **Ethics statement**

373 All procedures in this study regarding authentic SARS-CoV-2 virus were performed in
374 biosafety level 3 (BSL-3) facility, Medical School of Fudan University.

375 **Cell culture and transfection**

376 Vero E6 cells and HEK293T cells were cultured in DMEM supplemented with 10% FBS
377 at 37ºC in 5% CO_2 and the normal level of O_2. HEK293e cells were cultured in
378 serum-free FreeStyle 293 Medium (Invitrogen) with 120 rpm rotation at 37ºC in 5% CO_2
379 and the normal level of O_2. For transient overexpression in 293T and 293e, plasmids were
380 transfected using Lipofectamine 2000 (Invitrogen) according to the manufacture provided
381 protocol.

382 **Genomic receptor profiling**

383 To prepare SARS-CoV-2 S-ECD-hFc or control hFc containing condition medium,
384 pCMV-S-ECD-hFc or pCMV-secreted-hFc plasmid was transfected into 293e cells, and
385 condition medium was collected 4 days post transfection and filtered with 0.45um filter
386 for screening. To prepare receptor expressing cells, plasmids encoding 5054 human
387 membrane protein were individually co-transfected with CFP reporter vector (5:1) into
388 293e cells in 96 deep-well-plate. 2-5x10^4 membrane protein expressing cells per well
389 were collected 48hrs after transfection, washed once with PBS/2%FBS and incubated
390 with 1ml SARS-CoV-2 S-ECD or hFc control condition medium for 1hr on ice.
391 Supernatant was discarded after centrifugation and washed once with PBS/2%FBS, the
392 cells were then labelled with Anti-hFc-APC (Jackson Lab) antibody for 20min, and
393 washed once with PBS/2%FBS. The binding of S-ECD to the cells were measured by
394 HTS flow cytometry (BD CantoII). The flow data were analyzed with FlowJo software.
395 Relative binding of receptor (CFP^+ cells) to S-ECD-hFc compared with that to hFc
396 control were measured.

397 **Co-IP and Kd measurement**

398 Receptor expressing cells were lysed with RIPA buffer (Sigma) and centrifuged for
399 15min at 15000rpm at 4ºC, the cell lysate were collected. Purified hFc-tagged S-ECD
400 proteins (final concentration of 10ug/ml) were added into cell lysate together with
401 anti-FLAG beads, and incubated at 4ºC for overnight. Beads were washed three times
402 with the RIPA buffer, and the samples were prepared for western blot with anti-hFc or
403 anti-FLAG antibodies. For Kd measurement, receptor coding plasmid was co-transfected
404 with CFP reporter vector (5:1) into 293e cells. Cells were collected 48hr after transfection.
405 ~10^4 cells per well were used for binding with series diluted purified S-ECD-hFc proteins
406 as described in the experiment of Secretome Interaction Profiling. The flow data were
407 analyzed with FlowJo software. Ligand binding value at each ligand concentration was
408 normalized by equation of [(APC-MFI of CFP^+)-(APC-MFI of CFP^-)] - [(APC-MFI of
409 CFP^+)-(APC-MFI of CFP^-)] $_{\text{zero ligand concentration}}$. Kd and Bmax (maximum binding value)
410 were calculated with Prism8 software.

411 **Protein purification and western blot**

412 For purification of SARS-CoV-2 S-ECD-hFc, RBD-hFc, NTD-hFc, S2-hFc and
413 SARS-CoV S-ECD, the plasmids were transfected into 293e cells, and condition medium
414 was collected 4 days post transfection and filtered with 0.45um filter. hFc tagged proteins
415 were purified using Protein A affinity column and then desalted to PBS solution with
416 AKTA purifier system. Proteins were concentrated by 10KDa cutoff spin column
417 (Amicon). For western blot, samples was separated by SDS-PAGE gel and transferred to
418 nitrocellulose membrane. The membrane was labeled with the primary antibody and then
419 HRP-conjugated secondary antibody at suggested concentration, and detected by ECL kit
420 (Beyotime).

421 **ACE2 knockout 293T stable cell line**

422 ACE2 small guide RNA was constructed into pSLQ1651 (Addgene #51024) *(44)* with a

423 targeting sequence of CTTGGCCTGTTCCTCAATGGTGG. ACE2 sgRNA plasmid or
424 Cas9Bsd plasmid (Addgene #68343) *(45)* were co-transfected with psPAX2 and pMD2G
425 plasmids into 293T cells by Lipofectamine 2000 (Invitrogen) according to the
426 manufacture provided protocol. Lentivirus were collected 72hr post transfection to infect
427 293T cells. ACE2 KO 293T stable cell line were obtained by single cell dilution.

428 **Pseudotyped coronavirus packaging and infection**

429 For pesudotyped SARS-CoV-2, SARS-CoV and MERS-CoV, S protein encoding
430 pCDNA3.1 plasmids were mixed with pNL4-3.Luc.R vector separately with a ratio of 1:1,
431 and transfected into 293T cells using Lipofectamine 2000. Virus-containing supernatant
432 was collected 48-72 hours post-transfection and filtered through 0.45um PES membrane
433 filter (Millipore). For infection, cells were seeded into 96 well plate with ~2x104 cells per
434 well, 50ul virus-containing supernatant per well was added. Luciferase activities were
435 measured 48hr post infection with Bright-Lumi™ Firefly Luciferase Reporter Gene
436 Assay Kit (Beyotime, RG051M) and multifunctional microplate reader (TECAN 200pro).

437 **Authentic SARS-CoV-2 generation and infection**

438 SARS-CoV-2/MT020880.1 were expanded in Vero E6 cells. Cells were collected 50hr
439 post-infection and lysed by freeze-thaw method. Virus containing supernatants were
440 collected by centrifugation at ~2500xg for 10 minutes, and aliquot and stored at -80°C.
441 For infection, targeted cells were incubated with fresh medium diluted virus supernatant
442 at MOI of 0.1 for 48hrs. SARS-CoV-2 replication was examined by
443 immuno-fluorescence and flow cytometry with anti SARS-CoV-2 N protein antibody.

444 **Data analysis and statistics**

445 Gene Ontology Enrichment Analysis was performed by R bioconductor. For host-virus
446 interaction map, receptor expression in each tissues were obtained from human Protein
447 Atlas (https://www.proteinatlas.org/). mRNA expression level was normalized by
448 dividing the expression level with the Kd of each receptor. Virus infection rates of tissues

were obtained from the study published by Puelles et al. Cluster was performed with R package. For single cell sequencing (scRNA-seq) profile of the upper airway tract with COVID-19, the count, viral load and metadata are obtained from Magellan COVID-19 data explorer at https://digital.bihealth.org. Chi-square test and student's t-test were performed to compare receptor percentage and receptor expression value in different cell populations respectively. All tests were two sided. P value <0.05 was designated significance.

Reporting Summary:

Further information on research design is available in the Nature Research Reporting Summary linked to this paper.

Data availability:

Receptor expression levels in each tissues were obtained from human Protein Atlas (https://www.proteinatlas.org/). Single cell sequencing (scRNA-seq) profile of the upper airway tract with COVID-19 and the metadata were obtained from Magellan COVID-19 data explorer at https://digital.bihealth.org. All data supporting the findings of this study are available within the paper or in the extended data.

Methods References

44. Tzelepis, K. *et al.* A CRISPR Dropout Screen Identifies Genetic Vulnerabilities and Therapeutic Targets in Acute Myeloid Leukemia. *Cell Rep* 17, 1193-1205 (2016).
45. Chen, B. *et al.* Dynamic imaging of genomic loci in living human cells by an optimized CRISPR/Cas system. *Cell* 155, 1479-1491 (2013).

ACKNOWLEDGEMENTS

We thank Guy Riddihough of Life Science Editors for manuscript discussion and revision, and the staff in the Biosafety Level 3 Laboratory of Fudan University for experiments helping. This study was funded by the National Natural Science Foundation of China (projects 81873438 to Z.L., 81873922 to M.L.).

AUTHOR CONTRIBUTIONS

Z.L., M.L., Y.X., and G.X. conceived the project. Y.G., X.Z. and J.C with the help from J.Z., X.J., J.W., J.Y., X.Z., W.Y., Y.Z., performed receptor profiling, characterizing receptor-ligand interaction. M.L. H.G. and Y.W. performed virus related experiments with the help from G.S., X.J., F.L.. Z.L., M.L., J.W. Y.G., J.C. H.G. and Y.W. performed bioinformatics analysis and analyzed the data. Z.L., M.L., Y.X., G.X. and Y.Z. wrote the manuscript.

COMPETING INTERESTS

M.L., Z.L., Y.Z. H.G. and Y.X. are listed as inventors on a pending patent application for the newly identified S receptors described in this manuscript. The other authors declare no competing interests.